Earth and Planetary Science Letters 489 (2018) 72–83

Contents lists available at ScienceDirect

Earth and Planetary Science Letters

www.elsevier.com/locate/epsl

Slab interactions in 3-D subduction settings: The Philippine Sea Plate region

Adam F. Holt [a,*], Leigh H. Royden [a], Thorsten W. Becker [b], Claudio Faccenna [c]

[a] Department of Earth, Atmospheric and Planetary Sciences, M.I.T., Cambridge MA, United States
[b] Institute for Geophysics and Department of Geological Sciences, Jackson School of Geosciences, The University of Texas at Austin, Austin TX, United States
[c] Dipartimento Scienze, Università Roma TRE, Rome, Italy

ARTICLE INFO

Article history:
Received 8 September 2017
Received in revised form 23 December 2017
Accepted 20 February 2018
Available online xxxx
Editor: R. Bendick

Keywords:
double subduction
Philippine Sea Plate
subduction dynamics
plate velocities

ABSTRACT

The importance of slab–slab interactions is manifested in the kinematics and geometry of the Philippine Sea Plate and western Pacific subduction zones, and such interactions offer a dynamic basis for the first-order observations in this complex subduction setting. The westward subduction of the Pacific Sea Plate changes, along-strike, from single slab subduction beneath Japan, to a double-subduction setting where Pacific subduction beneath the Philippine Sea Plate occurs in tandem with westward subduction of the Philippine Sea Plate beneath Eurasia. Our 3-D numerical models show that there are fundamental differences between single slab systems and double slab systems where both subduction systems have the same vergence. We find that the observed kinematics and slab geometry of the Pacific–Philippine subduction can be understood by considering an along-strike transition from single to double subduction, and is largely independent from the detailed geometry of the Philippine Sea Plate. Important first order features include the relatively shallow slab dip, retreating/stationary trenches, and rapid subduction for single slab systems (Pacific Plate subducting under Japan), and front slabs within a double slab system (Philippine Sea Plate subducting at Ryukyu). In contrast, steep to overturned slab dips, advancing trench motion, and slower subduction occurs for rear slabs in a double slab setting (Pacific subducting at the Izu–Bonin–Mariana). This happens because of a relative build-up of pressure in the asthenosphere beneath the Philippine Sea Plate, where the asthenosphere is constrained between the converging Ryukyu and Izu–Bonin–Mariana slabs. When weak back-arc regions are included, slab–slab convergence rates slow and the middle (Philippine) plate extends, which leads to reduced pressure build up and reduced slab–slab coupling. Models without back-arcs, or with back-arc viscosities that are reduced by a factor of five, produce kinematics compatible with present-day observations.

© 2018 Elsevier B.V. All rights reserved.

1. Introduction

The Philippine Sea Plate is bounded to the west and east by west-dipping subduction zones (Fig. 1). It is the primary modern example of a plate bounded by two subducting slabs with the same polarity and thus presents the opportunity to interrogate subduction dynamics through slab–slab interactions. The two slabs can interact with each other via forces transmitted through the intervening plate and also through viscous forces exerted by subduction-induced mantle flow (e.g., Jagoutz et al., 2015). Understanding how such systems operate therefore has wide-ranging implications for the forces operating at subduction zones, and can be approached by utilizing dynamic modeling in conjunction with observations of subduction zone kinematics.

Holt et al. (2017) used 3-D numerical models to show that two proximal slabs with parallel trenches and the same subduction polarity exhibit strikingly different behavior from one another (Fig. 2). The slab that dips away from the middle plate ("front slab") has, for example, a low dip angle and a retreating trench. The slab that dips beneath the middle plate ("rear slab") has a high dip angle and a trench that advances. A number of 2-D numerical modeling studies have also shed light on the diversity of subduction kinematics that can be attributed to this configuration of double subduction (Mishin et al., 2008; Čížková and Bina, 2015; Faccenna et al., 2017).

We build upon these studies by considering subduction geometries that are applicable to the highly 3-D setting surrounding the Philippine Sea Plate. In this region of the western Pacific, the subduction segments exhibit strong kinematic variability both along-

* Corresponding author.
E-mail address: adamholt@mit.edu (A.F. Holt).

https://doi.org/10.1016/j.epsl.2018.02.024
0012-821X/© 2018 Elsevier B.V. All rights reserved.

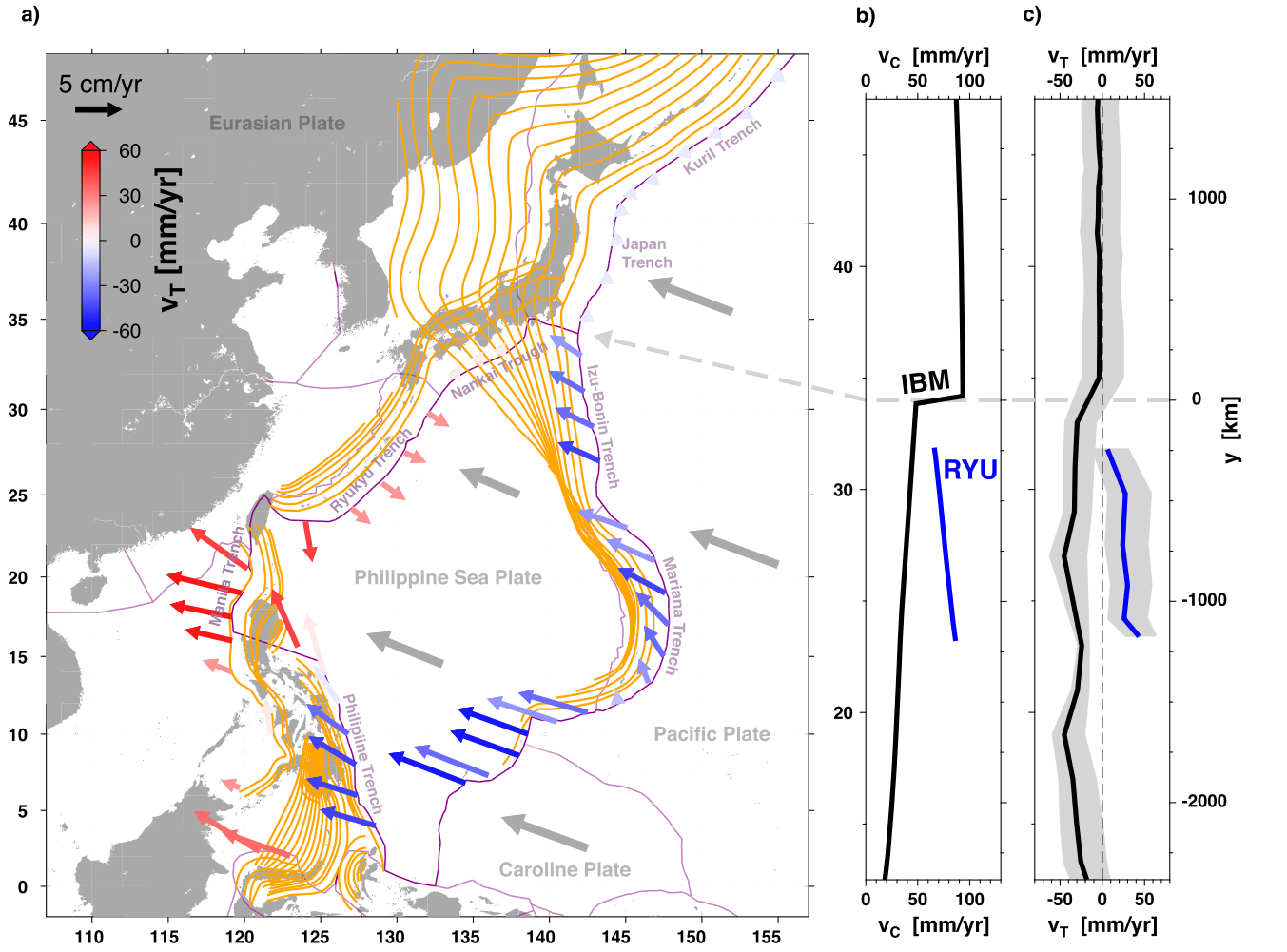

Fig. 1. Subduction kinematics in the Philippine Sea Plate region: a) Trench migration velocities in an absolute, spreading-aligned reference frame (Becker et al., 2015), relative plate motion vectors from MORVEL (DeMets et al., 2010) relative to Eurasia fixed, and RUM slab contours (Gudmundsson and Sambridge, 1998). Panel b) shows along-strike profiles of the magnitudes of the individual trench convergence rates at the Ryukyu (Philippine Sea Plate relative to Yangtze Plate) and Japan–Izu–Bonin–Mariana (Pacific Plate relative to Okhotsk and Philippine Sea plates) trenches (MORVEL). Panel c) shows the trench migration rates, V_T, at the subduction zones either side of the Philippine Sea Plate (black: Japan–Izu–Bonin–Mariana, "IBM", blue: Ryukyu, "RYU"). Negative and positive V_T corresponds to trench advance and retreat, respectively. In panel c), the solid lines are trench motions in the spreading-aligned reference frame. The upper (more positive) bound of the gray shading shows trench motions in a no-net-rotation (NNR) reference frame, and the lower bound shows motions in the hotspot (HS3) reference frame (Gripp and Gordon, 2002). (For interpretation of the colors in the figure(s), the reader is referred to the web version of this article.)

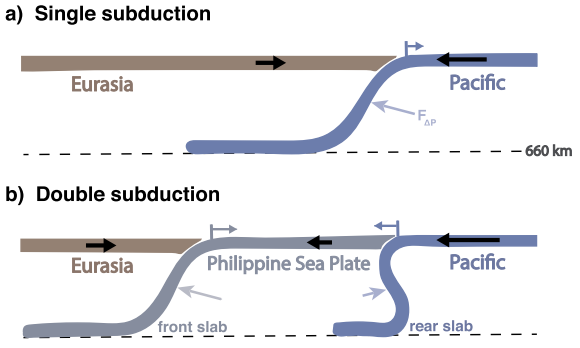

Fig. 2. Schematic illustration of the plate kinematics observed in the 3-D models of Holt et al. (2017): a) A "single subduction" model, and b) a "double subduction" model. Black arrows: plate velocities; dark colored arrows: trench migration velocities; light colored arrows: the force due to the across-slab asthenospheric pressure difference, ΔP.

strike and either side of the plate. We use observations from the Philippine Sea Plate and surrounding regions, coupled with 3-D dynamic modeling, to better constrain the forces and processes that operate around the margins of the Philippine Sea Plate, and those which dictate the along-strike change in behavior of the Pacific slab adjacent and north of the Philippine Sea Plate.

2. Tectonic overview

We first present a summary of the geometry and plate kinematics of the Philippine Sea Plate with a focus on the present-day. For an overview of the evolution of the Philippine Sea Plate since its inception (~55 Ma) we point the reader to the recent review of Lallemand (2016).

The Philippine Sea Plate is a relatively small plate (~2500 × 3250 km) consisting of oceanic lithosphere and sandwiched between the Pacific and Eurasia to the east and west and bounded, in a complex fashion, by the Sunda, Indo-Australian and Caroline plates to the south. Along its eastern margin, the Philippine Sea Plate overrides the Pacific Plate at the Izu–Bonin and Mariana trenches (Fig. 1). Along most of it western margin (Philippine, Ryukyu and Nankai boundaries), the Philippine Sea Plate subducts beneath a range of small-to-intermediate plates bordering the Eurasian Plate. In order to focus on the large-scale geodynamics, we group these plates together as the "Eurasian Plate" in our idealized models. The distance between the Ryukyu and Izu–

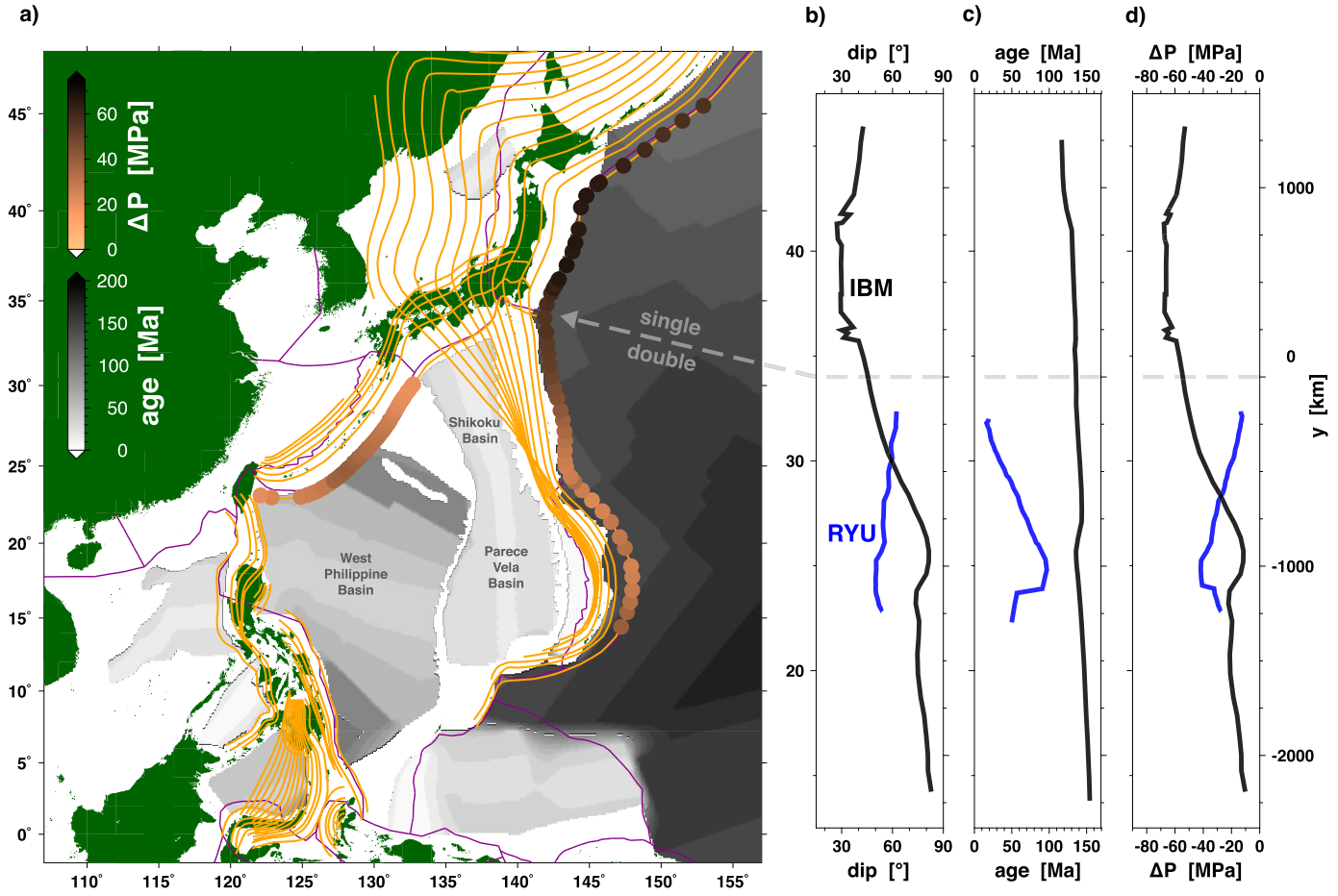

Fig. 3. Oceanic plate age, slab dip angles, and inferred across-slab pressure differences (ΔP) in the Philippine Sea Plate region: a) Map showing seafloor age distribution (Müller et al., 2008) and slab contours (Gudmundsson and Sambridge, 1998), b), along-strike variation in slab dip angle computed from the slab contours, c), age of oceanic plate subducting at the trench, and d), estimate of ΔP computed as described in the supplementary text using the dip (b) and age profiles (c). Computed ΔP values are also plotted in panel a) as colored points. The slab contours are at 50 km depth intervals, and the dips are computed at depths that are as deep as possible while the slab still exhibits along-strike continuity: For the Ryukyu/Nankai slab, dips are computed between 100 and 150 km, and for Japan–Izu–Bonin–Mariana, dip is computed between 200 and 300 km.

Bonin–Mariana trenches reaches ~2500 km in the center of the Philippine Sea Plate, and these trenches nearly meet at the northern tip of the Philippine Sea Plate where the Nankai Trough ends in central Japan. An exception to this double slab, "same-dip" geometry occurs along the western margin of the Philippine Sea Plate, where the South China Sea subducts beneath the Philippine Sea Plate at the Manila Trench.

Relative to eastern Eurasia, the Philippine Sea Plate presently moves to the WNW with a velocity of 6–11 cm/yr (e.g., DeMets et al., 2010; Kreemer et al., 2014). The velocity of the Pacific Plate is higher, at 9.5–11 cm/yr, and directed along approximately the same azimuth (Fig. 1). The Philippine Sea Plate is made up of three oceanic basins formed by sea floor spreading. Between ~54 and ~30 Ma, the West Philippine Basin opened and presently occupies greater than a third of the plate (e.g., Deschamps and Lallemand, 2002). Between ~30 and ~15 Ma, the Shikoku (North) and Parece-Vela basins (South) opened, and during this time the spreading orientation evolved from E–W to NE–SW, possibly in response to clock-wise plate rotation since 25–20 Ma (Hall et al., 1995; Sdrolias et al., 2004). Since 6–8 Ma, the Mariana Trough has undergone back-arc spreading at a full spreading rate of 20 (north) to 40 mm/yr (south) (e.g. Asada et al., 2007).

2.1. Pacific slabs (Izu–Bonin–Mariana Trench)

Convergence rates across the trench bounding the western margin of the Pacific Plate are highest north of the Philippine Sea Plate where the Pacific slab forms a single subduction boundary (Fig. 1b). In the MORVEL plate motion model, convergence rates reach ≈90 mm/yr at latitudes greater than ~34°N (DeMets et al., 2010). To the south, the total convergence rate between the Pacific and Eurasian plates increases to ≈120 mm/yr but is absorbed along the two west-dipping trenches on either side of the Philippine Sea Plate. At ~32°N; ≈45 mm/yr of convergence occurs along the Izu–Bonin Trench, between the Philippine and Pacific plates, and this decreases southward to ≈30 mm/yr at ~18°N (Fig. 1b).

The Pacific slab subducts to depths of at least the upper-lower mantle boundary along most of the eastern Philippine Sea Plate boundary and beneath Japan (e.g. Li et al., 2008). The dip of the Pacific slab changes markedly from north to south, with the change in slab dip broadly coinciding with where Pacific subduction transitions from beneath Japan to beneath the Philippine Sea Plate (Fig. 3). Dips computed from slab surface contours based on seismicity (Gudmundsson and Sambridge, 1998), between depths of 200 and 300 km, show slab dip increasing from ≈30° beneath Japan to ≈80° at the Mariana Trench (Fig. 3b) where the slab penetrates into the lower mantle (van der Hilst et al., 1991). In contrast, the shallowly dipping slab in the north lies flat at a depth of ~670 km, and extends westward along the transition zone for a lateral distance of ~2300 km (e.g., Liu et al., 2017).

2.2. Philippine slabs (Ryukyu Trench and Nankai Trough)

On the western margin of the Philippine Sea Plate, the average Ryukyu Trench convergence rate, between the Philippine and Eurasian plates, is ∼75 mm/yr and increases from north to south (Fig. 1b). The average rate is intermediate between the high Pacific trench convergence rate to the north of the Philippine Sea Plate, and the low rate at the Izu–Bonin–Mariana Trench. Further north at the Nankai Trough, estimates of the convergence rate vary between 31 mm/yr (Sella et al., 2002) and 60–70 mm/yr (Miyazaki and Heki, 2001; DeMets et al., 2010; Kreemer et al., 2014). The wide range of proposed convergence rates can be, in part, attributed to complications associated with removing intraplate deformation, and so we omit this segment from Fig. 1b.

The Ryukyu Trench and Nankai Trough constitute approximately half of the entire western Philippine Sea Plate boundary. At the Ryukyu Trench, the tomographic signal associated with the Philippine slab reaches a depth of ∼600 km and extends to a trench-perpendicular length of 700–1000 km (e.g. Li et al., 2008; Lallemand, 2016; Pownall et al., 2017). However, the continuity of various portions of the Ryukyu and Nankai/Shikoku slabs is debated: a sub-horizontal discontinuity may occur within the Ryukyu slab between 250 and 350 km (Lallemand et al., 2001; Pownall et al., 2017), and further north at the Nankai Trough the Shikoku slab may be absent at depths >∼100 km (Zhao et al., 2012; Huang et al., 2013; Cao et al., 2014). The average dip angle of the Ryukyu slab is ≈55°, and the dip exhibits an increase of ≈12° from south to north (Fig. 3b). The dip of the Shikoku slab is as low as 30°, possibly due to reduced negative buoyancy associated with Shikoku Basin subduction. Due to these complexities, we focus our large-scale analysis on the Philippine Sea Plate subducting at the Ryukyu Trench (latitudes <32.5°N).

2.3. Trench migration rates

There are important differences in the rate and direction of trench migration on either side of the northern portion of the Philippine Sea Plate. This is evidenced by the converging motion of these two trench systems, as the Philippine Sea Plate is progressively consumed at a rate of ∼60 mm/yr.

Along the Pacific trenches (i.e. where the Pacific Plate subducts: Japan–Izu–Bonin–Mariana), there are significant changes in the migration rate from north to south (Fig. 1c). While migration rates depend on the absolute plate motion model adopted as a reference, the pattern of along-strike variation is equivalent in all common reference frames. Going from single (Japan) to double slab subduction (Izu–Bonin–Mariana), the Pacific trench motion rate becomes more advancing by ∼35 mm/yr. In the suggested "generalized" reference frame constructed by minimizing the misfit between absolute plate motions and seafloor spreading orientations (Becker et al., 2015), for example, this corresponds to a switch from a near-stationary trench in the northern, single slab section to a Pacific trench that advances at ∼35 mm/yr in the double slab section. Advancing motion of the Izu–Bonin–Mariana Trench began at 10–5 Ma, after a period of trench retreat as the Philippine Sea Plate rotated clockwise (e.g., Le Pichon and Huchon, 1987; Hall, 2002; Faccenna et al., 2009).

The Ryukyu Trench is retreating in all commonly adopted reference frames, at a rate faster than the Japan Trench, and this is accommodated by back-arc extension in the Okinawa Trough. In the spreading-aligned reference frame, the Ryukyu Trench retreats at ∼30 mm/yr (Becker et al., 2015).

2.4. Southern Philippine Sea Plate

To the south, the Philippine Sea Plate is juxtaposed against the Sunda, Caroline, and Indo-Australian plates by a combination of juvenile subduction zones, a slow spreading ridge, and a diffuse strike-slip boundary (Lallemand, 2016). While it is established that the Caroline Plate is mechanically coupled to Pacific Plate motion, the large-scale structure of the southeastern Philippine Sea Plate boundary is unclear as seismicity is limited to crustal depths.

South of Taiwan, the polarity of subduction is reversed at the ∼800 km long Manila Trench, where the South China Sea subducts beneath the Philippine Sea Plate with a trench-perpendicular slab length of ∼400 km. Further south, the Philippine Sea Plate reverts back to west-directed subduction at the ∼1000 km long Philippine Trench, where the slab length is typically <350 km (e.g. Wu et al., 2016). Because of the complex nature of the southern/southwestern subduction boundaries, and the low trench-perpendicular slab lengths (i.e. slab pull) relative to Ryukyu, we focus primarily on the subduction systems bounding the northern half of the plate.

3. Double subduction modeling

2-D modeling studies have illuminated the wide range of kinematics associated with double slab subduction in a configuration where the slabs dip in the same direction (e.g., Mishin et al., 2008). In particular, Čížková and Bina (2015) showed that the presence of an additional subduction zone (Ryukyu) ahead of the Pacific slab may be responsible for the advancing motion of the modern Izu–Bonin–Mariana Trench, and Faccenna et al. (2017) proposed that the switch from Izu–Bonin–Mariana Trench retreat to advance is associated with the re-establishment of double subduction after Ryukyu slab break-off at 10–5 Ma. Alternative mechanisms proposed previously for this trench advance include Pacific Plate aging (Faccenna et al., 2009) and large-scale plate geometry (Nagel et al., 2008).

Holt et al. (2017) used numerical models to investigate 3-D double subduction systems with two parallel trenches, and compared their behavior to that of single slab systems. Significant kinematic variability exists between the double subduction system with equivalently dipping slabs and the single slab system. In such double slab systems, we refer to the slab that subducts away from the middle plate as the "front" slab, and the slab that subducts under the middle plate as the "rear" slab (Fig. 2b). The front slab exhibits kinematics that are comparable to single slab models with equivalent mechanical properties: i.e. Trench retreat, a dip angle of <90°, and a similar convergence rate. Both the front slab (double slab system) and the single slab exhibit a mantle pressure which is negative above the slab and positive beneath the slab, which results in a pressure force directed towards the mantle wedge (e.g. Fig. 2a). The rear slab behavior is fundamentally different. Positive pressure build-up in the asthenosphere between the two slabs causes the sign of the across-slab pressure difference to switch, which results in a pressure force that is directed towards the sub-slab region at asthenospheric depths (Fig. 2b). In conjunction with this, extensional stress within the middle plate pulls the shallow part of the rear slab toward the middle plate. These coupled effects result in a rear slab that dips >90°, undergoes trench advance (e.g. Čížková and Bina, 2015), and has a relatively low convergence rate.

In comparing Pacific–Philippine Sea Plate tectonics to these idealized double subduction models, the northern, Japan portion of the Pacific subduction system is analogous to a single slab system. Southward, the system that bounds the northern half of the Philippine Sea plate is analogous to a double subduction system, with front (Ryukyu/Nankai) and rear (Izu–Bonin–Mariana) slabs. While the principles governing the behavior in a parallel trench system can therefore be used to build intuition about the first-order processes, the geometry of the Philippine Sea Plate is, however, more complex: It contains an along-strike transition from single to dou-

ble slab subduction, and a slab separation distance that increases from near-zero in the north to greater than 2000 km across the central Philippine Sea Plate. We therefore build on the results of Holt et al. (2017) by considering subduction geometries more appropriate for the Philippine Sea Plate. This allows us to examine the degree to which this configuration can induce the observed kinematics, and isolate the primary forces governing such behavior.

4. Numerical model setup

We use the 3-D finite-element code CitcomCU to solve the conservation equations that govern convection in an incompressible viscous fluid with negligible inertia (Moresi and Gurnis, 1996; Zhong, 2006). Our modeling strategy is to search for simplified models that can reconcile the kinematic observations and therefore give insight into the important dynamic processes. The general setup is similar to that of the "same-dip" double subduction model presented in Holt et al. (2017), but with some major geometrical, and minor mechanical, differences outlined below.

We use purely viscous models to target first order processes, with a density and viscosity that depends solely on the compositional field that defines the locations of the lithospheric plates and crustal layers. Relative to Holt et al. (2017), the only rheological difference is the absence of a strong lithospheric core, which we have removed because the Philippine Sea Plate does not act as a rigid body (the Mariana back-arc spreads at rates of 20–40 mm/yr). The 80 km thick lithospheric plates are 85 kg/m^3 denser and are a factor 500 more viscous than the asthenosphere (density = 3300 kg/m^3, viscosity = 2×10^{20} Pas). The asthenospheric viscosity was chosen to yield a single slab convergence rate of ~90 mm/yr, similar to that observed in Japan (Fig. 1b). A 15 km thick, weak "crustal" layer is inserted on top of the subducting plates to decouple the subducting and overriding plates. This layer has the same density as the lithosphere and a viscosity equivalent to that of the asthenosphere. In the fore-arc region of the Pacific–Philippine Sea Plate boundary, the Philippine Sea Plate crustal layer is tapered from full to zero thickness between distances of 330 and 150 km from the trench, in order to ensure that the Philippine Sea Plate remains stable as an overriding plate (i.e., is not dragged into the asthenosphere by the Pacific Plate). To enable relative motion between the modeled Philippine Sea and Eurasian plates, we insert a weak "shear zone" at the edge of the Philippine Sea Plate (Fig. 4). This channel is 55 km wide, cuts through the lithosphere, and has a density and viscosity equal to that of the asthenosphere.

The primary modifications in the double subduction models are geometrical: We increase the trench-parallel dimension of the model domain (from 2640 km to 3300 km), to allow a wider Pacific trench (i.e., Japan–Izu–Bonin–Mariana) that extends across the entire domain. Therefore, toroidal flow cannot occur around the wide subducting Pacific slab, but can be induced around the Ryukyu slab (Fig. 4). Due to its large along-strike length of ~5500 km, we consider this an appropriate way to parameterize Pacific subduction. The height of the model domain is 660 km, the trench-perpendicular length is 7920 km, and all boundaries are mechanically free slip. The front (Ryukyu) slab has an initial depth of 330 km, shallower than in Holt et al. (2017) and motivated by work suggesting that Ryukyu subduction was interrupted by slab break-off at ~10 Ma (Lallemand et al., 2001). The rear (Izu–Bonin–Mariana) slab has an initial depth of 500 km. Both slabs are initiated with a radius of curvature of 150 km and a dip angle of 70°. Different initial dip angles are explored in Holt et al. (2017), where it is shown that a value of 70° leads to slabs that bend backwards (i.e. away from the upper plate), as observed for the Japan, Ryukyu and Izu–Bonin slabs.

In addition to a model with parallel trenches (Fig. 4a) and an initial trench separation of 2000 km, we explore the effect

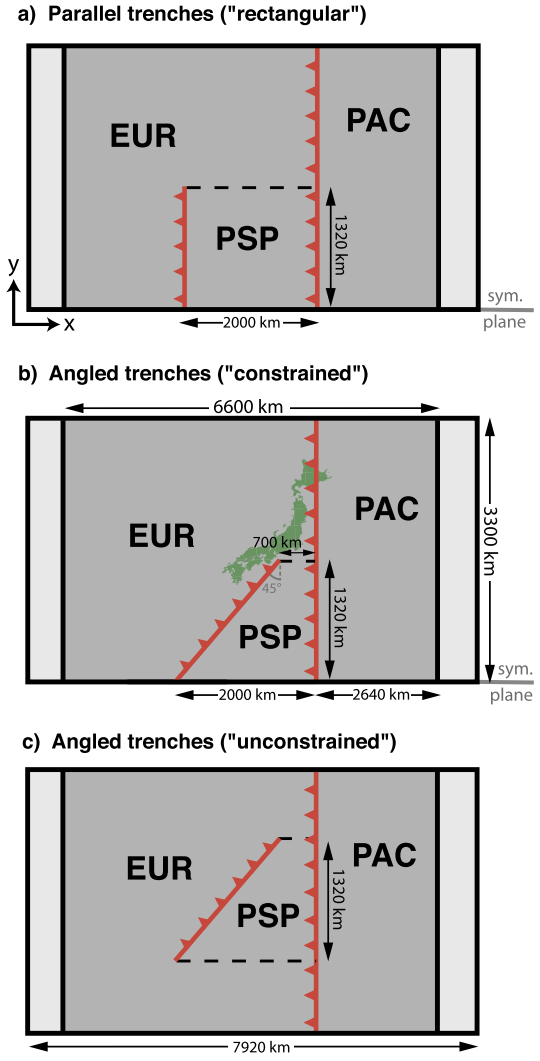

Fig. 4. Illustration of the initial conditions for the three double slab model geometries. The dashed black lines denote the location of weak zones that are used to decouple the Philippine Sea and Eurasian plates. They cut trough the entire lithosphere and have an initial width of 55 km. Note that the parallel trench and "constrained" angled trench models have a plane of symmetry in the trench-perpendicular direction. (EUR = Eurasian Plate, PSP = Philippine Sea Plate, PAC = Pacific Plate.)

of oblique trenches. The trench–trench angle is initially set to 45° and the initial trench–trench distance varies from 700 km at the edge of the modeled Philippine Sea Plate to 2000 km in the center (Figs. 4b, 4c). Because the plate boundary configuration in the southern portion of the Philippine Sea Plate is complex, we use two simplified end-member geometries for the southern portion of the plate (Fig. 4): A case where the trenches remain far apart at the southern end of a triangle-shaped Philippine Sea Plate and the intervening asthenosphere is not tightly constrained ("unconstrained" subduction), and a case where the trenches nearly meet at the end of a diamond-shaped Philippine Sea Plate and the slabs constrain the asthenosphere ("constrained" subduction). In the supporting information, we have included a schematic figure showing the "constrained" model geometry in detail (Fig. S1) and a table containing all parameter values (Table S1).

In addition to our reference models, we also examine the dynamic effect of the presence of weak back-arc regions. Further details about how this is parameterized are given in Section 5.3.

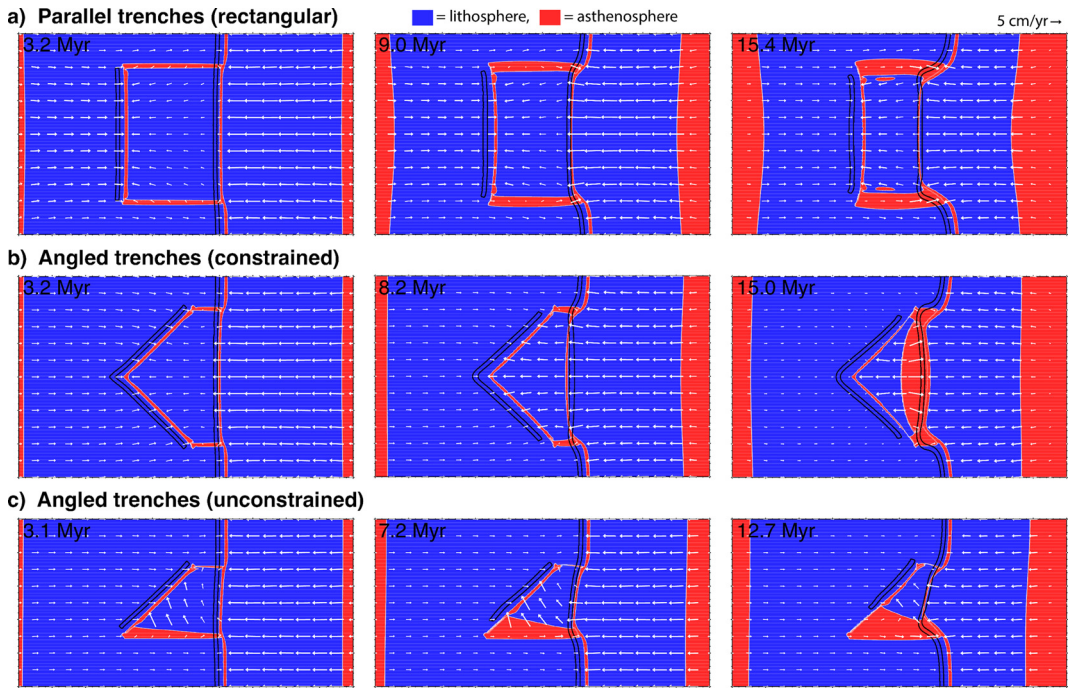

Fig. 5. Evolution of the plate velocities and plate boundary shapes for the three model geometries: a) rectangular, b) constrained, and c) unconstrained cases. A sub-section of the model domain, centered on the model Philippine Sea Plate, is shown. The (horizontal) plate velocities are extracted within the lithosphere at a depth of 25 km, in order to avoid the 15 km thick, weak crustal layers. The black contours show the location of the subducting slabs at mid-mantle depth (330 km).

5. Modeling results

For convenience, we refer to the plates and trenches in our models using the geographic names of the plates and trenches they are intended to represent (left-most plate: Eurasian Plate, mid-plate: Philippine Sea Plate, right-most: Pacific Plate, etc.). The three subduction geometries described in the previous section are shorthanded to "rectangular" (Figs. 4a, 5a), "constrained" (Figs. 4b, 5b), and "unconstrained" (Figs. 4c, 5c).

Unless otherwise indicated, the reference frame discussed is that of the model boundaries. In this frame, the average position of the Pacific Trench is nearly fixed because the Pacific slab extends to the side of the model domain and so asthenosphere cannot flow around Pacific slab edge. Conservation of mass requires that the average position of the Pacific slab moves eastward at ∼1/8 of the Pacific Plate velocity (lithosphere thickness divided by upper mantle thickness).

5.1. Common features

After the models have evolved from their various initial conditions, a number of features are common to all geometries. The velocity of the Pacific Plate is the most rapid and that of Eurasia is, in general, the slowest (Fig. 5). Convergence between the Pacific and Eurasian plates is rapid, at 90–130 mm/yr. Across the northern, single slab portion of the system, this is entirely absorbed by subduction of the Pacific Plate beneath Eurasia at ∼90 mm/yr. Across the double slab portion of the system, the Pacific Plate subducts relatively slowly at 20–55 mm/yr. Subduction of the Philippine Sea Plate beneath Eurasia (Ryukyu Trench), at ∼70 mm/yr, absorbs most of the Pacific–Eurasia convergence in the double slab section, and leads to the gradual consumption of the plate. (Plate velocities in a Eurasia-fixed reference frame are presented in Fig. S2.)

The motions of the trenches change systematically along-strike (Figs. 6, 7). Along the single slab portion of the system (Pacific–Eurasia boundary) the Pacific/Japan Trench retreats to the east. Along the double slab portion of the system, the Pacific/Izu–Bonin Trench advances to the west while the Ryukyu Trench retreats at a rate similar to that of the single slab portion of the Pacific trench (Japan). In the constrained model at 8.2 Myr, for example, the Japan and Ryukyu trenches retreat at ∼20 mm/yr while the Izu–Bonin Trench advances at ∼45 mm/yr (Figs. 6b, 7c). This along-strike variation in trench motion results in a strongly curved Pacific–Philippine Sea Plate boundary in the models, the center of which progressively protrudes out towards Eurasia (Fig. 5).

The slab dip angle, computed between depths of 170 and 330 km, also exhibits strong variability. The Pacific slab has a moderate, near-constant dip of ∼70° in the single slab portion of the system. Where it subducts beneath the Philippine Sea Plate in the double slab portion of the system, the slab steepens and can become overturned, with a dip that reaches ∼120° in the constrained case (Figs. 6c, 7d). The western (Ryukyu) slab is more shallowly dipping, with a dip of ∼55° in the central portion of the Philippine Sea Plate and almost 70° at the northern boundary.

There is also systematic variation in the dynamic pressure difference across the slab. The pressure difference, ΔP, as computed by subtracting the dynamic pressure on the underside side of the slab from that on the mantle wedge side of the slab, is negative (~ -20 MPa) across the Pacific slab in the northern, single slab portion of the system (Figs. 6d, 7e). Where the Pacific slab subducts beneath the Philippine Sea Plate, ΔP is less negative, and in some cases positive: In the constrained subduction geometry, ΔP reaches a maximum of $+10$ MPa. This occurs due to positive pressure build-up in the asthenosphere beneath the Philippine Sea Plate, which also drives asthenosphere to flow from beneath the plate and towards the negatively pressurized single slab mantle wedge region (Fig. 8). To the west, the Ryukyu slab exhibits highly negative ΔP, between -30 and -15 MPa for the constrained subduction geometry.

Overall, where there is a single Pacific slab, the system behaves like the single subduction system of Fig. 2a, with rapid convergence, a retreating trench, moderate slab dip, and negative ΔP. Where two slabs are present, the system behaves like the double subduction system of Fig. 2b: While the front/western slab

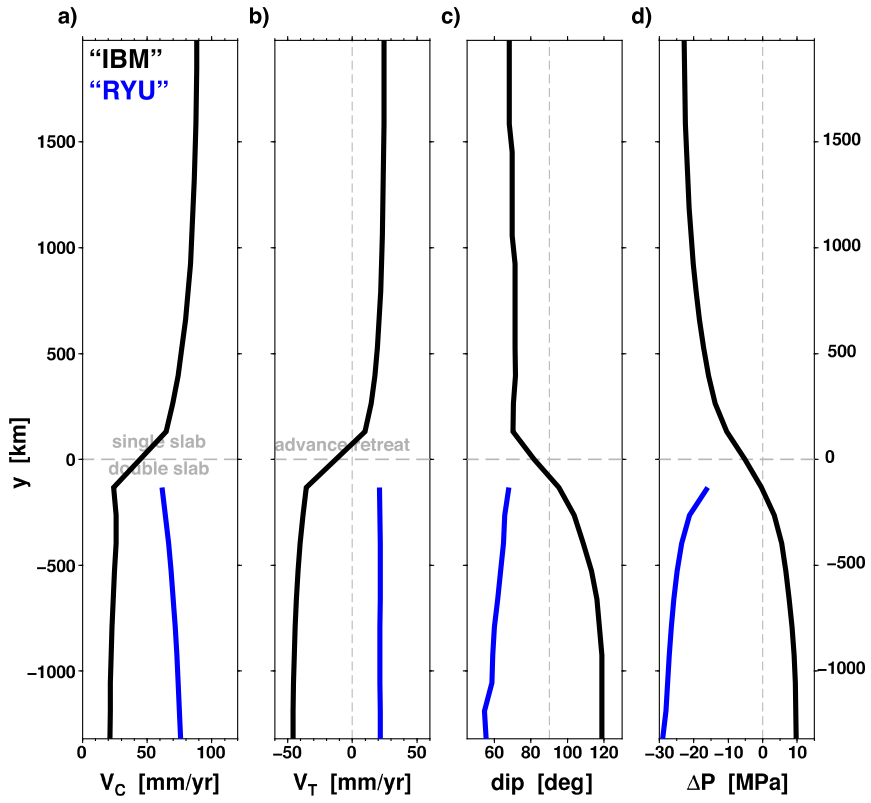

Fig. 6. Along strike variation in subduction kinematics for the model with angled trenches and a constrained Philippine Sea Plate, at the time-step shown in Fig. 5b. Panels show, a) trench convergence rates, b) trench migration rates (negative V_T = trench advance), c) slab dip angle (computed between depths of 170 and 330 km, i.e. centered on 250 km), and d) across-slab pressure difference. The across-slab pressure difference is computed from pressures extracted at two points in the model, both at depths of 250 km and 50 km from either side of the subducting slab surface (defined by a boundary in the compositional field which tracks the lithosphere–asthenosphere boundary).

exhibits behavior similar to a single slab, the rear/eastern slab exhibits slow convergence, trench advance, a steep/overturned slab dip, and near-neutral/positive ΔP.

5.2. Variability among model results

Clear differences between the three model geometries occur in the plate velocity direction and the shape of the plate boundaries (Fig. 5). The unconstrained case yields a Philippine Sea Plate that moves approximately northwest, while in all other models the Philippine Sea Plate moves east–west. The biggest difference, however, occurs in the constrained model geometry, where the Pacific and Philippine Sea plates separate at a model time of ∼11 Myr (Fig. 5b). This occurs as the extensional stress at the plate boundary induces a trench-perpendicular extension rate, in the crustal channel, that exceeds the Izu–Bonin–Mariana Trench advance rate. After separation, the trenches on either side of the Philippine Sea Plate are no longer forced to converge at the rate of subduction of the Philippine Sea Plate; the motion of the Izu–Bonin–Mariana Trench changes from advance to retreat (Fig. S3). In plan view, this causes the Philippine Sea–Pacific Plate boundary to develop the opposite sense of curvature (i.e. the central portion of the boundary curves away from Eurasia, as observed in the western Pacific). From this time onward, this model behaves much like the models containing weak back-arcs, described in Section 5.3.

The three model geometries exhibit differences in the magnitude of positive asthenospheric pressure beneath the Philippine Sea Plate, which induce differences in subduction kinematics (Fig. 7). The constrained geometry has the greatest sub-Philippine Sea Plate pressure (∼20 MPa), because mantle flow can only evacuate the central region by flowing through narrow boundary regions at the edge of the Philippine Sea Plate. The rectangular geometry exhibits intermediate values at ∼10 MPa, while the unconstrained case has near-zero average pressure in this inter-slab region (Fig. 7a). The sub-Philippine Sea Plate pressure affects the asthenospheric pressure difference across the slabs on either side of the Philippine Sea Plate, with a higher pressure creating a more negative ΔP across the front slab and a more positive ΔP across the rear slab. The constrained geometry therefore has the most negative ΔP for the front slab (Ryukyu) and most positive ΔP for rear slab (Izu–Bonin–Mariana). In contrast, the adjacent single subduction section is relatively unaffected by the build up of pressure beneath the Philippine Sea Plate.

Because slab dip correlates with ΔP, the various models exhibit different slab dips across the double subduction portions of the systems (Fig. 7). The steepest, most overturned dips of the Pacific (rear) slab thus occur in the constrained subduction case (120°, as compared to 95° for the rectangular model and ≤90° for the unconstrained model). Relative to the constrained case, the other geometries also exhibit reduced along-strike variation in convergence and trench motion rates, but do exhibit the same sense of along-strike variation. For instance, while single slab rates are similar, the Pacific trench advance rate in the double slab section is greater in the constrained case (≈45 mm/yr) than in the rectangular model (≈25 mm/yr).

The frontal trench (Ryukyu) generally exhibits more subdued variations between the model geometries. All cases have average Ryukyu convergence rates of ∼70 mm/yr, trench retreat rates of 20–40 mm/yr, and relatively low slab dip angles of 55–70° (Fig. 7).

5.3. Weak back-arcs

Examining the effect of weak "back-arcs" is motivated by the presence of back-arc spreading within the Philippine Sea Plate (Mariana) and inherited weakness from previous spreading

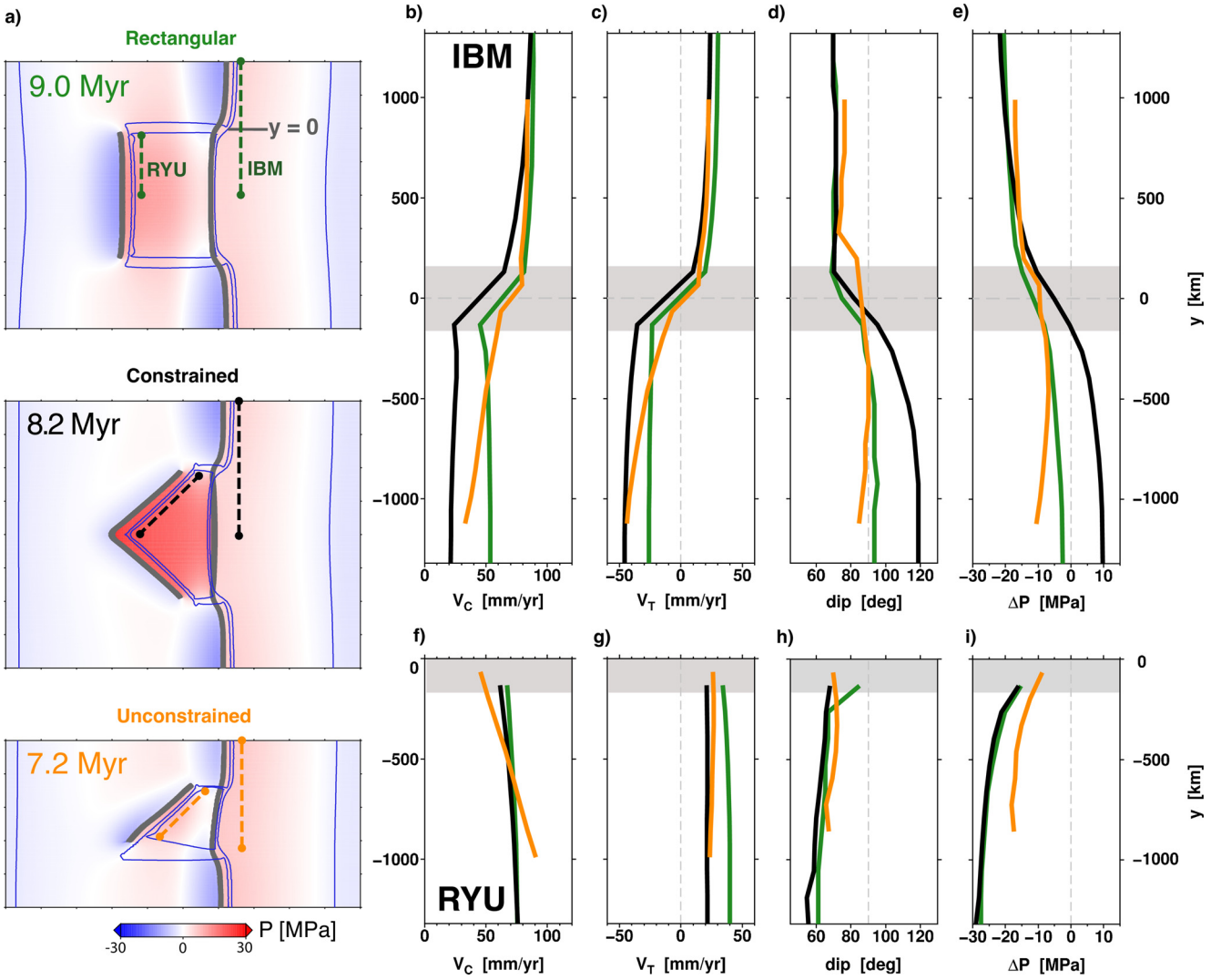

Fig. 7. Comparison of subduction kinematics for three double slab geometries. Leftmost panel, a), shows mantle (dynamic) pressure and slab shapes at mid-mantle depths ($z = 330$ km), and locations of profiles plotted in the other panels (dashed lines). b–e) Profiles of subduction properties for the modeled Pacific trenches (Japan–Izu–Bonin–Mariana), equivalent as those presented in Fig. 6 for the constrained model. f–i) Profiles of the same subduction properties for the modeled Ryukyu Trench/Nankai Trough.

episodes (Shikoku, Parece-Vela). We parameterize these regions by reducing the lithospheric viscosity in the back-arc regions to different values in "weak" ($\eta_{\text{back-arc}} = 0.2\eta_{\text{plate}}$) and "weakest" ($\eta_{\text{back-arc}} = 0.05\eta_{\text{plate}}$) cases, in regions located 300 km from the trench and initially 300 km wide.

Intuitively, the lower the strength of the back-arc region, the greater the rate at which the Philippine Sea Plate extends (Figs. 9, S4). At a model time of 7.7 Myr, the weakest back-arc region extends at a rate of ~55 mm/yr, on the order of the convergence rate at western Pacific trenches. Because the Ryukyu and Izu–Bonin–Mariana trenches now converge at a greatly reduced rate, there is little build up of positive asthenospheric pressure ahead of the Izu–Bonin–Mariana slab (0–5 MPa), and little transmission of extensional stress across the Philippine Sea Plate to the Pacific plate boundary. Through both the asthenosphere and the lithosphere, the Ryukyu and Pacific slabs are thus now decoupled and so behave similar to slabs in single slab systems. The rear (Pacific) trench now retreats and has a rapid convergence rate, has a slab dip lower than 90°, and the central portion curves away from the Eurasian Plate (in plan-view). While the model with moderate strength back-arcs ($0.2\eta_{\text{plate}}$) also exhibits reduced magnitude double slab kinematics, the kinematics are closer to that of the reference case without weakening (Fig. 9).

The front, Ryukyu slab is less affected by the presence of the weak back-arcs. For this slab, the most significant effect of back-arc weakening is a reduction in the convergence rate at the edge of the Philippine Sea Plate, which increases the along-strike variation in convergence rate (Fig. 9f).

6. Discussion and conclusions

All of the single-to-double slab geometries investigated in our numerical models exhibit similar behavior, comparable to the geometry and kinematics observed adjacent to and north of the Philippine Sea Plate (cf. Figs. 1, 7). These results indicate that the first-order subduction kinematics around the Philippine Sea Plate are controlled by the along-strike transition from single to double subduction and are not strongly dependent on the detailed shape of the Philippine Sea Plate. The observed kinematics occur primarily due to the relative build-up of dynamic mantle pressure beneath the middle (Philippine Sea) plate in the double slab region. This pressure build-up drives the asthenosphere to flow out from the double slab into the single slab region (Fig. 8). Such flow is consistent with shear wave splitting observations that have been interpreted to indicate trench-parallel asthenospheric flow in the Ryukyu sub-slab region (Anglin and Fouch, 2005), and with

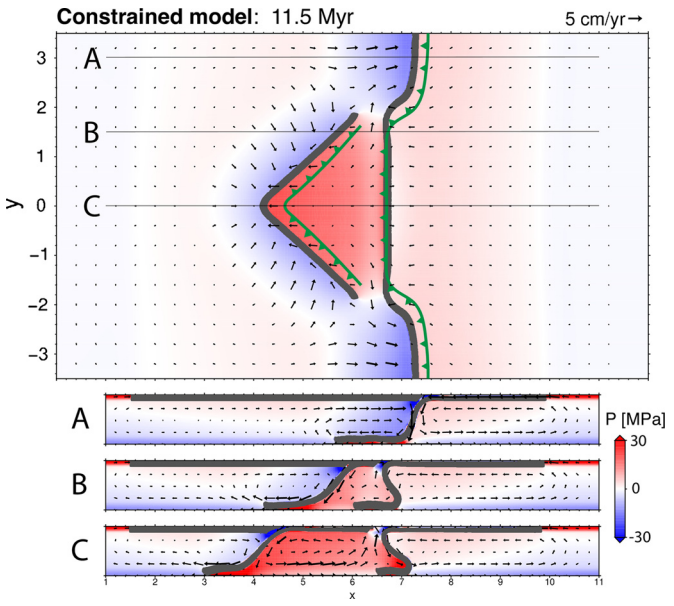

Fig. 8. Mantle (dynamic) pressure and velocity field for a representative time-step of the constrained model. The upper panel shows a horizontal slice of dynamic pressure, with mantle flow vectors, at a model depth of 330 km. The surface location of the trenches is shown in dark green. Lower panels are vertical cross sections that are at locations in the single slab region (A), near the edge of the modeled Philippine Sea Plate (B), and through the center of the Philippine Sea Plate (C).

isotopic compositions of southern Mariana arc lavas that suggest asthenospheric outflow from beneath the Philippine Sea Plate in the south (Ribeiro et al., 2017).

At asthenospheric depths, elevated dynamic pressure acts to push the slabs away from each other and at shallower, lithospheric depths, extensional stress within the Philippine Sea Plate pulls the trenches together (Holt et al., 2017). This results in a negative across-slab pressure difference at the Japan (single) and Ryukyu (front) slabs, and a near-neutral/positive pressure difference across the Izu–Bonin–Mariana (rear) slabs. As observed, a change in Pacific subduction from a single to a double slab setting therefore results an increase in slab dip, a switch towards trench advance (e.g. Carlson and Melia, 1984; Čížková and Bina, 2015) and hence a reduction in the convergence rate (Faccenna et al., 2007). Also in agreement with observations, the modeled Ryukyu slab exhibits trench retreat, has a rapid convergence rate that decreases to the north, and a relatively low slab dip. The occurrence of these characteristics in the Ryukyu/Nankai and Japan–Izu–Bonin–Mariana systems therefore suggests similar dynamic processes act within these regions as in our numerical models, and emphasizes the important role that subduction-induced mantle pressure plays in dictating subduction kinematics (e.g. Gerault et al., 2012).

The magnitude of the dynamic pressure in the mantle beneath the Philippine Sea Plate is a function of how confined the mantle is between the bounding slabs and how rapidly the slabs converge. The constrained model exhibits the greatest pressure build-up, because asthenosphere evacuates this region through only the narrow gaps between the two slabs (Fig. 8). To first order, this is consistent with tomographic images that show the Pacific and Philippine Sea Plate slabs nearly overlapping at the northern end of the Philippine Sea Plate (e.g., Li et al., 2008; Nakajima et al., 2009; Fukao and Obayashi, 2013). However, we note that there are potential discontinuities within various sections of both the Ryukyu (e.g., Lallemand et al., 2001; Zhao et al., 2012; Huang et al., 2013) and Pacific slabs (e.g., Miller et al., 2004, 2006), and so uncertainty remains regarding the precise degree of sub-Philippine Sea Plate mantle confinement and therefore the optimal model configuration and level of mantle pressurization. While our main goal here is a conceptual understanding, the quantitative agreement between the results of the constrained model and many observations is good. The transition from single to double Pacific slab subduction is associated with an observed convergence rate reduction of ∼50 mm/yr (taken at 500 km either side of the single-to-double transition), compatible with an equivalent reduction in our models (cf. Figs. 1, 6). While the shift in model trench velocity is lower (∼60 mm/yr) than observed (∼35 mm/yr), the inclusion of moderately weak back-arcs reduces the along-strike change in trench velocity to ∼45 mm/yr. For the Ryukyu slab, our constrained model produces trench retreat magnitudes (∼20 mm/yr) that are in line with the values observed within a range of absolute plate motion reference frames (10–55 mm/yr) and, as observed in plate motion models, a convergence rate that decreases by 15–25 mm/yr towards the northern edge of the Philippine Sea Plate.

6.1. Slab dip angles

Despite an equivalent sense and magnitude of along-strike variation, the modeled dip angles for the Pacific Plate (Fig. 6: 70–120°) are consistently higher than those observed (Fig. 2: 30–80°). This can be attributed to the use of reduced trench-perpendicular lengths for the modeled Pacific and Eurasian plates (2640 km and 2000–4000 km, respectively). Slab dip correlates with the pressure difference across the slab, which is approximately equal to slab buoyancy times the cosine of slab dip (e.g. Holt et al., 2017). Because dynamic pressure scales with plate length and plate width (see supplementary material of Jagoutz et al., 2015), smaller subducting plates produce higher slab dips (e.g., Fig. 3 of Holt et al., 2017). Estimates of the pressure difference computed directly from the slab dip angles and subducting plate ages observed in the region, as shown in Fig. 3d and explained in detail in the appendix, are indeed greater magnitude than those observed in our models (e.g. Fig. 6d). This supports the inference that our model geometries underestimate the magnitude of the pressure difference across the Pacific slab. In contrast, the model plate lengths for the Philippine Sea Plate are comparable to reality and thus produce a good match to the observed dip angle.

A component of this dip angle discrepancy may also be associated with slab morphology attained prior to our period of interest. Because we compare Philippine Sea Plate observations with our models at a model time of ∼8 Ma, we implicitly assume that the slabs had a constant dip angle at ∼8 Ma. However, the slab dip angle may have inherited significant variability by this time. In particular, if the Izu–Bonin–Mariana Trench underwent >2000 km of trench retreat since the Eocene (e.g., Seno and Maruyama, 1984; Hall, 2002), the slab dip may have been lower than the 70° initially imposed in our models. Another example of pre-existing slab morphology that may be in part driven by additional processes is the cusp-like shape of the Pacific subduction zones, centered on Japan (i.e., Izu–Japan–Kuril trenches). Here, in addition to the Japan to Izu–Bonin–Mariana dip angle increase to the south, the Pacific slab dip angle exhibits a more moderate increase towards the north (Fig. 3). Coupled double subduction may have only operated since the cessation of Shikoku/Parece-Vela spreading (e.g., Section 5.3) and re-initiation of Ryukyu subduction (Faccenna et al., 2017), and thus overprinted a preexisting symmetric cusp with greater dips in the south (Izu–Bonin–Mariana: dip ≤80°) than the north (Kuril–Kamchatka: dip ≤50°).

6.2. Lower mantle effects

We have neglected the presence of a viscous lower mantle in order to simplify the model setup. The Mariana slab penetrates to depths of ∼1100 km in the viscous lower mantle (van

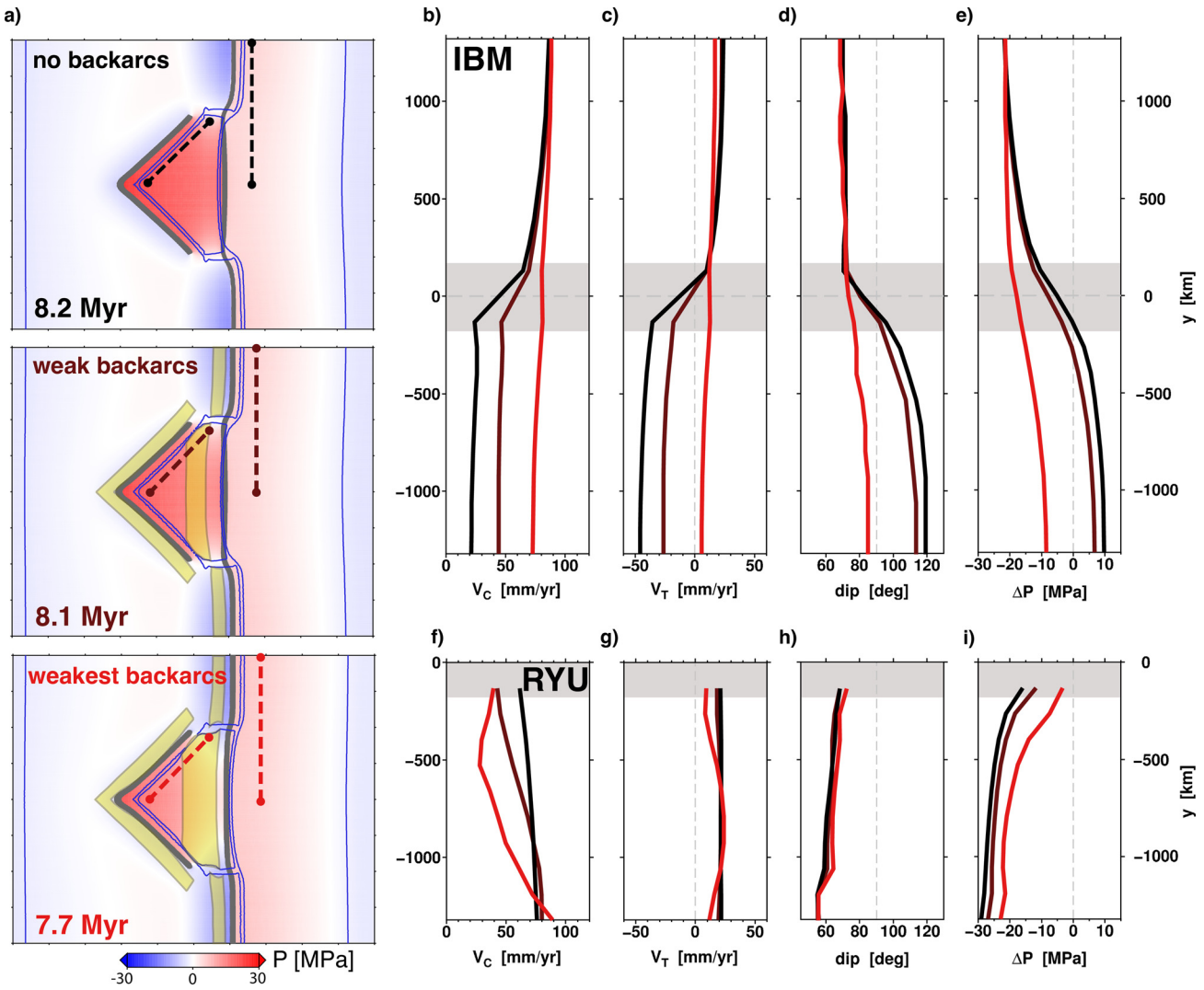

Fig. 9. Comparison of subduction kinematics for constrained geometry models with the inclusion of weakened back-arcs. "Weak" ($\eta_{\text{back-arc}} = 0.2\eta_{\text{plate}}$) and "weakest" back-arc cases ($\eta_{\text{back-arc}} = 0.05\eta_{\text{plate}}$) are compared with the reference case (e.g., Fig. 5b). Leftmost panel (a) shows mantle (dynamic) pressure and slab shapes at mid-mantle depths ($z = 330$ km), profile locations (dashed lines), and back-arc locations (yellow shaded regions). b–e) Profiles of subduction properties for the modeled Pacific trenches (Japan–Izu–Bonin–Mariana), and, f–i), profiles for the modeled Ryukyu Trench.

der Hilst et al., 1991), and Mariana slab anchoring may exert a control on the temporal evolution of trench motions in the region (van der Hilst and Seno, 1993). While our focus is on the present-day geodynamics, 3-D models that contain a viscous lower mantle are thus required to test the degree of control that slab anchoring had on Philippine Sea Plate evolution since its inception. For the present-day configuration, our setup is appropriate for the slabs that bound the northern half of the Philippine Sea Plate or subduct beneath Japan, where tomographic images show the slabs flattening in the mid-mantle (e.g., Li et al., 2008; Fukao and Obayashi, 2013).

6.3. Back-arcs

The inclusion of weak back-arcs in our models leads to enhanced stretching of the overriding plate during subduction, which, in a double slab setting, reduces the rate that the two slabs converge at. This leads to a reduction of the positive dynamic pressure build-up beneath the plate (Holt et al., 2017), which causes the pressure difference across the rear, Pacific slab to become more negative. At shallower depths, there is a coupled reduction in the west-directed pull on the Izu–Bonin–Mariana Trench, as the extensional stress in the Philippine Sea Plate is reduced. Back-arc weakening thus modifies the force balance on the Pacific slab such that it becomes similar to a single subducting slab (Fig. 2a). As suggested by Billen (2015), back-arc weakening can therefore decouple the double slab system into two, largely independent, single subduction zones: In our "weakest" back-arc model, the model Izu–Bonin–Mariana Trench becomes retreating and the convergence increases to a rate similar to the adjacent single slab segment (Fig. 9). As is observed in our "weakest" back-arc model, the average full spreading rate in the Shikoku and Parece-Vela basins (30–15 Ma) was comparable to the convergence rate at the Izu–Bonin–Mariana Trench at this time, both on the order of 50 mm/yr (e.g., Sdrolias and Müller, 2006). Slab decoupling due to the presence of active back-arc spreading thus provides a mechanism for retreat of the Izu–Bonin–Mariana Trench at ~30–15 Ma, despite the likely persistence of a double subduction geometry (e.g. Faccenna et al., 2009). Back-arc spreading also enables the Philippine Sea Plate to be preserved through geological time by the reducing the, otherwise rapid (Jagoutz et al., 2015), rate of convergence between the two slabs (equivalent to the rate of plate consumption).

While the linear viscosity models used here allow us to establish the first-order dynamic relationships, models with lithospheric plasticity and thermal effects may allow the spatio-temporal rela-

tionship between back-arc spreading history and double subduction to be further studied. The modulation of slab–slab interactions by plastic yielding in the back-arc could lead to an episodic/cyclical Philippine Sea Plate evolution: Convergence between the slabs leads to a build-up of dynamic pressure beneath and extensional stress across the Philippine Sea Plate. This could trigger extension within the Philippine Sea Plate, slowing the rate of slab convergence and reducing the asthenospheric pressure and extensional stress (e.g. Fig. 9). As the extensional stress in the lithosphere reduces, the spreading ridges may shut down and heal thermally, allowing the slabs to again become coupled.

Presently, the double slab system may be in a phase of intermediate coupling as back-arc spreading occurs over a limited region at the Mariana Trough and, northward, the Izu–Bonin arc is extending but not spreading (e.g. Taylor et al., 1991). The double slab system may thus be evolving into a state with margin-wide back-arc extension and decoupled subduction zones. In addition to the reference case (no back-arcs), the model with moderately weak back-arcs ($\eta_{\text{back-arc}} = 0.2\eta_{\text{plate}}$), and moderate slab coupling appears to be a reasonable analog for the present-day. While the weakest back-arc case ($\eta_{\text{back-arc}} = 0.05\eta_{\text{plate}}$) appears compatible with the region during margin-wide spreading (~30–15 Ma), it does not exhibit the required slab–slab coupling to explain present-day observations. This suggests a lower bound for the effective, integrated viscous strength of the present-day back-arc region of 5% of that of the oceanic plate interior.

Our results demonstrate the important role of along-strike mantle pressure variation for producing the subduction kinematics observed in the northwest Pacific. Furthermore, this work adds weight to recent studies that emphasize the importance of slab–slab interactions (e.g., Jagoutz et al., 2015; Čížková and Bina, 2015; Király et al., 2016; Holt et al., 2017; Király et al., 2018), and illustrates the utility of basic subduction principles in untangling subduction dynamics within complex subduction geometries. While additional model complexity may bring our results into even closer agreement with observations, the first-order observations and, by inference, the dominant processes at work in the Philippine Sea Plate region are well-explained by an along-strike transition from single to double subduction.

Acknowledgements

We thank Serge Lallemand for helpful discussions about Philippine Sea Plate tectonics, and our two anonymous reviewers for their comments which helped to improve the presentation of this manuscript. We also thank the original authors and CIG (geodynamics.org) for providing CitcomCU. The modified code version used in this study is available upon request to the authors. Most figures in this paper were made using the Generic Mapping Tools (Wessel et al., 2013).

Appendix A. Supplementary material

Supplementary material related to this article can be found online at https://doi.org/10.1016/j.epsl.2018.02.024.

References

Anglin, D.K., Fouch, M.J., 2005. Seismic anisotropy in the Izu–Bonin subduction system. Geophys. Res. Lett. 32. https://doi.org/10.1029/2005GL022714.

Asada, M., Deschamps, A., Fujiwara, T., Nakamura, Y., 2007. Submarine lava flow emplacement and faulting in the axial valley of two morphologically distinct spreading segments of the Mariana back-arc basin from Wadatsumi side-scan sonar images. Geochem. Geophys. Geosyst. 8 (4). https://doi.org/10.1029/2006GC001418.

Becker, T.W., Schaeffer, A.J., Lebedev, S., Conrad, C.P., 2015. Toward a generalized plate motion reference frame. Geophys. Res. Lett. 42, 3188–3196. 2015.

Billen, M., 2015. Geodynamics: double dip. Nat. Geosci. 8. https://doi.org/10.1038/ngeo2431.

Cao, L., Wang, Z., Wu, S., Gao, X., 2014. A new model of slab tear of the subducting Philippine Sea Plate associated with Kyushu–Palau Ridge subduction. Tectonophysics 636, 158–169. https://doi.org/10.1016/j.tecto.2014.08.012.

Carlson, R.L., Melia, P.J., 1984. Subduction hinge migration. Tectonophysics 102, 399–411.

Čížková, H., Bina, C., 2015. Geodynamics of trench advance: insights from a Philippine-sea-style geometry. Earth Planet. Sci. Lett. 430, 408–415.

DeMets, C., Gordon, R.G., Argus, D.F., 2010. Geologically current plate motions. Geophys. J. Int. 181, 1–80. https://doi.org/10.1111/j.1365-246X.2010.04491.x.

Deschamps, A., Lallemand, S., 2002. The West Philippine Basin: an Eocene to early Oligocene back arc basin opened between two opposed subduction zones. J. Geophys. Res. 107 (B12), 2322. https://doi.org/10.1029/2001JB001706.

Faccenna, C., Di Giuseppe, E., Funiciello, F., Lallemand, S., van Hunen, J., 2009. Control of seafloor aging on the migration of the Izu–Bonin–Mariana trench. Earth Planet. Sci. Lett. 288, 386–398.

Faccenna, C., Heuret, A., Funiciello, F., Lallemand, S., Becker, T.W., 2007. Predicting trench and plate motion from the dynamics of a strong slab. Earth Planet. Sci. Lett. 257, 29–36.

Faccenna, C., Holt, A.F., Becker, T.W., Royden, L.H., Lallemand, S., 2017. Dynamics of the Ryukyu/Izu–Bonin–Marianas double subduction system. Tectonophysics. https://doi.org/10.1016/j.tecto.2017.08.011.

Fukao, Y., Obayashi, M., 2013. Subducted slabs stagnated above, penetrating through, and trapped below the 660 km discontinuity. J. Geophys. Res. 118, 5920–5938.

Gerault, M., Becker, T.W., Kaus, B.J.P., Faccenna, C., Moresi, L., Husson, L., 2012. The role of slabs and oceanic plate geometries in the net rotation of the lithosphere, trench motions, and slab return flow. Geochem. Geophys. Geosyst. 13. https://doi.org/10.1029/2011GC003934.

Gripp, A.E., Gordon, R.G., 2002. Young tracks of hotspots and current plate velocities. Geophys. J. Int. 150, 321–361.

Gudmundsson, O., Sambridge, M., 1998. A regionalized upper mantle (RUM) seismic model. J. Geophys. Res. 103, 7121–7136.

Hall, R., 2002. Cenozoic geological and plate tectonic evolution of SE Asia and the SW Pacific: compute-based reconstructions, model and animations. J. Asian Earth Sci. 20 (4), 353–431.

Hall, R., Ali, J.R., Anderson, C.D., Baker, S.J., 1995. Origin and motion history of the Philippine Sea Plate. Tectonophysics 251, 229–250.

Holt, A.F., Royden, L.H., Becker, T.W., 2017. The dynamics of double slab subduction. Geophys. J. Int. 209, 250–265.

Huang, Z., Zhao, D., Hasegawa, A., Umino, N., Park, J.H., Kang, I.B., 2013. Aseismic deep subduction of the Philippine Sea Plate and slab window. J. Asian Earth Sci. 75, 83–94.

Jagoutz, O., Royden, L., Holt, A.F., Becker, T.W., 2015. Anomalously fast convergence of India and Eurasia caused by double subduction. Nat. Geosci. 8. https://doi.org/10.1038/ngeo2418.

Király, Á., Capitanio, F.A., Funiciello, F., Faccenna, C., 2016. Subduction zone interaction: controls on arcuate belts. Geology 44 (9). https://doi.org/10.1130/G37912.1.

Király, Á., Holt, A.F., Funiciello, F., Faccenna, C., Capitanio, F., 2018. Modeling slab–slab interactions: dynamics of outward dipping double-sided subduction systems. Geochem. Geophys. Geosyst. https://doi.org/10.1002/2017GC007199. In press.

Kreemer, C., Blewitt, G., Klein, E.C., 2014. A geodetic plate motion and Global Strain Rate Model. Geochem. Geophys. Geosyst. 7. https://doi.org/10.1002/2014GC005407.

Lallemand, S., Font, Y., Bijwaard, H., Kao, H., 2001. New insights on 3-D plates interaction near Taiwan from tomography and tectonic implications. Tectonophysics 335 (3–4), 229–253.

Lallemand, S., 2016. Philippine Sea Plate inception, evolution, and consumption with special emphasis on the early stages of Izu–Bonin–Mariana subduction. Prog. Earth Planet. Sci. 3 (15). https://doi.org/10.1186/s40645-016-0085-6.

Le Pichon, X., Huchon, P., 1987. Central Japan triple junction revisited. Tectonics 6, 35–45.

Li, C., van der Hilst, R.D., Engdahl, R.E., Burdick, S., 2008. A new global model for P wave speed variations in Earth's mantle. Geochem. Geophys. Geosyst. 9 (5). https://doi.org/10.1029/2007GC001806.

Liu, X., Zhao, D., Li, S., Wei, W., 2017. Age of the subducting Pacific slab beneath East Asia and its geodynamic implications. Earth Planet. Sci. Lett. 464, 166–174.

Miller, M.S., Kennett, B.L.N., Lister, G.S., 2004. Imaging changes in morphology, geometry, and physical properties of the subducting Pacific Plate along the Izu–Bonin–Mariana arc. Earth Planet. Sci. Lett. 224 (3–4), 363–370.

Miller, M.S., Kennett, B.L.N., Toy, V., 2006. Spatial and temporal evolution of the subducting Pacific Plate structure along the Western Pacific margin. J. Geophys. Res. 111. https://doi.org/10.1029/2005JB003705.

Mishin, Y.A., Gerya, T.V., Burg, J.P., Connolly, J.A.D., 2008. Dynamics of double subduction: numerical modeling. Phys. Earth Planet. Inter. 171, 280–295.

Miyazaki, S., Heki, K., 2001. Crustal velocity field of southwest Japan: subduction and arc–arc collision. J. Geophys. Res. 101, 4305–4326.

Moresi, L.N., Gurnis, M., 1996. Constraints on the lateral strength of slabs from three-dimensional dynamic flow models. Earth Planet. Sci. Lett. 138, 15–28. https://doi.org/10.1016/0012-821X(95)00221-W.

Müller, R.D., Sdrolias, M., Gaina, C., Roest, W.R., 2008. Age, spreading rates and spreading symmetry of the world's ocean crust. Geochem. Geophys. Geosyst. 9, Q04006. https://doi.org/10.1029/2007GC001743.

Nagel, T.J., Ryan, W.B.F., Malinervo, A., Buck, W.R., 2008. Pacific trench motions controlled by the asymmetric plate configuration. Tectonics 27. https://doi.org/10.1029/2007TC002183.

Nakajima, J., Hirose, F., Hasagawa, A., 2009. Seismotectonics beneath the Tokyo metropolitan area, Japan: effect of slab–slab contact and overlap on seismicity. J. Geophys. Res. 114. https://doi.org/10.1029/2008JB006101.

Ribeiro, J.M., Stern, R.J., Martinez, F., Woodhead, J., Chen, M., Ohara, Y., 2017. Asthenospheric outflow from the shrinking Philippine Sea Plate: evidence from Hf–Nd isotopes of southern Mariana lavas. Earth Planet. Sci. Lett. 478, 258–271.

Sdrolias, M., Müller, R.D., 2006. Controls on back-arc basin formation. Geochem. Geophys. Geosyst. 7. https://doi.org/10.1029/2005GC001090.

Sdrolias, M., Roest, W.R., Müller, R.D., 2004. An expression of Philippine Sea Plate rotation: the Parece Vela and Shikoku Basins. Tectonophysics 394, 69–86.

Sella, G.F., Dixon, T.H., Mao, A., 2002. REVEL: a model for recent plate velocities from space geodesy. J. Geophys. Res. 107. https://doi.org/10.1029/2000JB000972.

Seno, T., Maruyama, S., 1984. Paleogeographic reconstruction and origin of the Philippine Sea. Tectonophysics 102 (1–4), 53–84.

Taylor, B., Klaus, A., Brown, G.R., Moore, G.F., Okamura, Y., Murakami, F., 1991. Structural development of Sumisu Rift, Izu–Bonin Arc. J. Geophys. Res. 96, 16113–16129.

Pownall, J.M., Lister, G.S., Spakman, W., 2017. Reconstructing subducted oceanic lithosphere by 'reverse-engineering' slab geometries: the northern Philippine Sea Plate. Tectonics 36 (9), 1814–1834. https://doi.org/10.1002/2017TC004686.

van der Hilst, R.D., Engdahl, E.R., Spakman, W., Nolet, G., 1991. Tomographic imaging of subducted lithosphere beneath northwest Pacific Island arcs. Nature 353, 37–43.

van der Hilst, R.D., Seno, T., 1993. Effects of relative plate motion on the deep structure and penetration depth of slabs below the Izu–Bonin and Mariana island arcs. Earth Planet. Sci. Lett. 120, 395–407.

Wessel, P., Smith, W.H.F., Scharroo, R., Luis, J., Wobbe, F., 2013. Generic mapping tools: improved version released. EOS, Trans. Am. Geophys. Union 94, 409–410.

Wu, J., Suppe, J., Lu, R., Kanda, R., 2016. Philippine Sea and East Asian plate tectonics since 52 Ma constrained by new subducted slab reconstruction methods. J. Geophys. Res. 121, 4670–4741.

Zhao, D., Yanada, T., Hasegawa, A., Umino, N., Wei, W., 2012. Imaging the subducting slabs and mantle upwelling under the Japan Islands. Geophys. J. Int. 190, 816–828.

Zhong, S., 2006. Constraints on thermochemical convection of the mantle from plume heat flux, plume excess temperature and upper mantle temperature. J. Geophys. Res. 111. https://doi.org/10.1029/2005JB003972.